Dielectric relaxation of the amorphous ices

2008 J. Phys.: Condens. Matter 20 244115

(http://iopscience.iop.org/0953-8984/20/24/244115)

J. Phys.: Condens. Matter **20** (2008) 244115 (9pp) doi:10.1088/0953-8984/20/24/244115

Dielectric relaxation of the amorphous ices

Ove Andersson

Department of Physics, Umeå University, 901 87 Umeå, Sweden

Received 28 February 2008
Published 29 May 2008
Online at stacks.iop.org/JPhysCM/20/244115

Abstract

The dielectric properties of the low and high density amorphous ices are discussed in terms of those for supercooled water and crystalline ices, and also used to evaluate the transition behaviour upon pressure cycling at 130 K. The dielectric relaxation of the high density amorphous ice is described well by the symmetrical Cole–Cole function with an almost pressure independent relaxation time $\tau \sim 2$ s at 133 K and a relaxation time distribution factor of 0.7. At the high to low density amorphous ice transition, the dielectric relaxation time increases by about two orders of magnitude despite a ∼30% decrease in density, and τ of the low density amorphous ice is in the range 10^2–10^3 s at 130 K. The relaxation time behaviour of the high density amorphous ice is similar to that of supercooled liquid water, whereas τ of the low density amorphous ice appears to be prolonged by the ice rules, in correspondence to that of the crystalline ices.

(Some figures in this article are in colour only in the electronic version)

1. Introduction

Liquid water is one of the most difficult states to supercool to form a vitreous state. Bulk water inevitably crystallizes, but it is possible to form amorphous states, e.g. by deposition of micron-sized droplets or water vapour onto a plate kept at liquid nitrogen temperature. The states formed by these methods are referred to as hyperquenched glassy water (HGW) and amorphous solid water (ASW), respectively. In 1984 Mishima *et al* [1] discovered a new path to produce amorphous solid water through pressure induced amorphization (PIA), and a year later [2] they observed a transition between two amorphous solid states. The phenomenon of PIA in ice, and properties of these amorphous ices and their relation to ASW and HGW, have been recently reviewed [3, 4]. These interesting findings by Mishima *et al* [1, 2] raised the question of whether or not the two amorphous states, which are referred to as high and low density amorphous ice, have two liquid counterparts. A firm identification of two liquid water states would lead to great progress in the understanding of water's overall behaviour, since it would make a second critical point probable and, thus, provide an origin for many anomalies in water's properties. However, despite numerous investigations of the amorphous states, there are only a limited number of experimental studies that have reported indications of a glass transition for the two amorphous ices that are produced under pressure. Moreover, after a scrutiny of all experimental studies, Koza *et al* [5] concluded that these glass-transition-like features might be caused by other reasons than a glass transition. Further information concerning the properties of the amorphous ices, and especially the nature of the amorphous states, are vital to progress the understanding of water.

The amorphous ices are produced at low temperatures initially through a pressure induced collapse of hexagonal ice (Ih) or cubic ice (Ic). Water's high density amorph, HDA ice, is made by pressurizing ice Ih or ice Ic in the temperature range 77–140 K to ∼1.5 GPa. Since the transformation is time dependent [6], with a time constant which depends on temperature and pressure, the HDAs produced in this manner differ in properties depending upon the temperature, pressure, and time profiles used in the preparation. Recent studies have suggested that the term HDA is generic and refers to all amorphous solids produced by pressure-collapse of ice Ih and ice Ic at different temperature and time conditions [7–9]. An ultimate, presumably highest density 'HDA', originally denoted 'VHDA' [10] and lately also 'vHDA' or 'rHDA', seems to have been produced when the amorphous solid formed by pressurizing ice Ih at 77 K was heated to 160 K while under a pressure near 1 GPa [10]. It has recently been shown that only VHDA is homogeneous [9]. Thus, HDAs formed under other conditions could be constrained states, possibly consisting partly of distorted nanosized crystals, that relax and/or become fully amorphized when heated, yielding the VHDA state. The other name suggested for this state, i.e. relaxed HDA or rHDA,

would be consistent with the relaxation picture on heating. In this work, the high density amorphous state was produced by slow pressurization of ice Ih at 130 K to 1.3 GPa. Since the relaxation time of the high density amorph is short under these conditions and it does not relax further on heating [11–13], it should be in the ultimate densified form. Therefore, it is here referred to as rHDA to emphasize that it is different from the HDA produced by pressurization of ice Ih at liquid nitrogen temperature. (In view of the heterogeneous character of HDA, it has been argued that it should not be referred to as a state of the amorphous water network [9].)

Water's low density amorph is produced by heating of HDA at atmospheric pressure or at elevated pressures of ∼0.05 GPa and below [7]. Using a heating rate of ∼3 K min^{-1} at atmospheric pressure, HDA transforms to low density amorphous ice (LDA) at ∼117 K [14]. However, if the high density amorph is produced by isothermal pressurization at higher temperatures, or annealed at high temperatures and pressures, typically in the range 120–150 K at 1 GPa, after production at 77 K, it becomes more dense and stable, approaching the vHDA/rHDA state [10, 13], and transforms to LDA at higher temperatures on heating near atmospheric pressures. Neutron and x-ray scattering studies have shown that HDA also converts to LDA isothermally at different temperatures, beginning at ∼95 K at atmospheric pressure [15]. An alternative path to produce LDA is to isothermally depressurize (r)HDA ice at ∼130 K to low pressures [16, 17]. As the pressure can be rapidly changed and stabilized, this path is preferred for studies that are time consuming, requiring stable pressure and temperature conditions for an hour, as in the case of the low frequency dielectric study discussed here.

The structures of the HDA and LDA states have been the subject of several investigations [15, 18–21], but the descriptions based on the diffraction data have differed somewhat. The amorphous states appear to exhibit a tetrahedral arrangement with fully hydrogen bonded network, but there is one important distinguishing feature in the nearest neighbour oxygen–oxygen coordination. This concerns 'interstitial' non-hydrogen bonded molecules, which resides just outside, in the range 3.1–3.3 Å, the four tetrahedrally coordinated water molecules [18, 19]. At atmospheric pressure, the HDA state produced by pressurization at 77 K has about one (interstitial) non-hydrogen bonded molecule and vHDA/rHDA about two molecules in the first neighbour shell, taken to be between 2.3 and 3.3 Å [18], whereas the LDA state exhibits no such interstitial molecules. Klotz *et al* [20] have discussed their results for HDA ice in terms of increasing interpenetrating hydrogen networks with increasing pressure, but Martonak *et al* [22] have argued that this is incompatible with their results of molecular dynamics simulations of HDA and vHDA/rHDA ice.

This work provides new data and a more comprehensive analysis of the dielectric behaviour of LDA ice than that previously reported [23]. It also discusses the previously reported [11, 12], as well as new, dielectric results for rHDA. As shown here, the dielectric properties give, together with previously reported thermal properties [17, 24], a unified and consistent picture of the LDA and rHDA ices, where the former exhibits a crystalline response similar to those of ices Ih and Ic and the latter exhibits properties similar to those of liquid water.

2. Experimental details

The study was performed by using a parallel plate dielectric cell of nominally 149 pF air capacitance. The capacitor consisted of six plates, separated from each other by polyetheretherketone (PEEK) spacers. The capacitor was placed inside a 37 mm internal diameter Teflon container, which itself fitted inside the high pressure cylinder of internal diameter 45 mm.

The Teflon container, with the dielectric cell, was filled with about 25 ml of water purified by using Milli-Q® Ultrapure WaterSystems, sealed with a Teflon lid and the piston inserted. The whole assembly was transferred to a vacuum chamber and load was applied using a 5 MN hydraulic press. The pressure in the cell was determined from the ratio of load to area, to which a correction for friction was applied. This correction had been previously established in a separate room temperature experiment by using the pressure dependence of the resistance of a manganin wire. The pressure of the hydraulic oil used to push the piston into the cylinder was computer-controlled at the desired rate of increase or decrease. The temperature of the pressure vessel was varied by using a built-in helium cryostat equipped with a heater [25].The data are accurate to within ±0.05 GPa for pressure (at 1 GPa and 100 K) and ±0.3 K for temperature.

The complex capacitance was measured using a Solartron 1260 impedance analyser above 100 Hz, whereas an HP33120A function generator was used below to provide a sinusoidally varying signal over the sample capacitor and a reference capacitor placed in series. The voltages over the capacitors were measured simultaneously by two HP3457A voltmeters during at least one period (100 points), and the capacitance and conductance of the sample were determined for each frequency. The set-up is the same as has been described previously [26], but with a new function generator and electronics. The geometric capacitance of the capacitor was determined by using the known high frequency dielectric permittivity of ice Ih of 3.1 at low pressures, and the change with pressure was approximately taken into account assuming isotropic compression of all the materials between the plates (and also the PEEK spacers).

3. Results

The rHDA state was produced by isothermal pressurization of ice Ih up to 1.3 GPa at 130 K using 0.17 GPa h^{-1} rate. The absence of an abrupt pressure/volume change and a simultaneous temperature increase, which would occur at a transition to a high pressure crystalline ice [27], showed that the amorphization process was successful. Since the amorph was produced by relatively slow pressurization at 130 K, where it become fully relaxed within less than one minute [11–13], this production procedure yields the fully relaxed high density

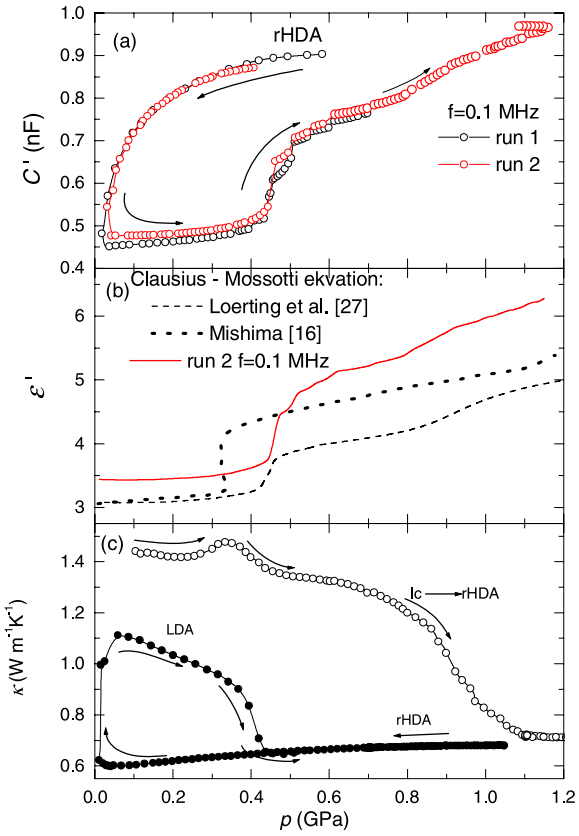

Figure 1. (a) Capacitance as a function of decreasing pressure at ∼130 K for two samples initially in the rHDA state, and subsequent pressure increase. (b) High frequency dielectric permittivity calculated assuming isotropic compression of all the material between the electrodes, and values calculated using the Clausius–Mossotti relation (see text for details). (c) Thermal conductivity as a function of pressure: (●) results on pressure decrease for a sample initially in the rHDA state, and subsequent pressure increase at 130 K [17], (○) results during pressure increase at 130 K for a mixture of initially 'HDA and ice Ic' [29].

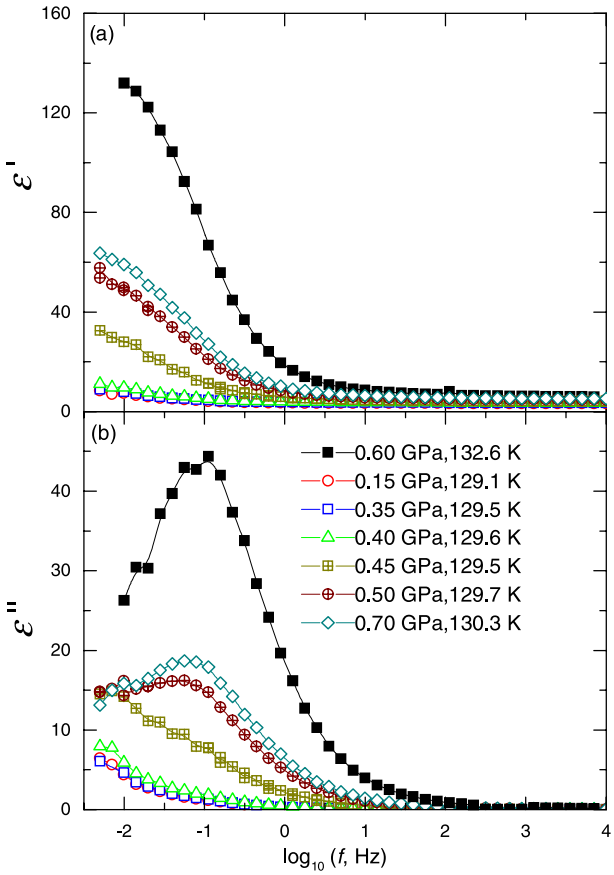

Figure 2. Dielectric permittivity and loss as a function of frequency on depressurization (solid symbol) and subsequent pressurization after the pressure had been decreased to ∼0.03 GPa.

amorphous state rHDA (or VHDA). Two samples of rHDA were produced by this procedure and depressurized to 1 GPa at 130 K. One of these was then heated to ∼140 K at 1 GPa, and cooled back to 130 K in 6 h. The results for the high frequency capacitance on cooling were the same as those on heating (within less than 0.5 %), which shows that the sample did not densify further, i.e. it was already in the rHDA state after the production at 130 K. Subsequently, the sample was depressurized to 0.6 GPa, where it was cooled to 110 K during the night, and heated up to 130 K in 1.5 h in the morning (labelled run 1 in figure 1(a)). The other rHDA sample (labelled run 2) was cooled isobarically to 110 K at 1 GPa over 9 h. The pressure was thereafter lowered to 0.4 GPa at about 0.15 GPa h^{-1} and, subsequently, the temperature was increased isobarically from 110 to 130 K in 1.5 h. The data for the real part of the high frequency (0.1 MHz) capacitance C' for these two samples of different thermal histories were then recorded during pressure decrease from 0.6 or 0.4 GPa at 130 K to 0.03 GPa, followed by an increase up to 1.1 GPa (figure 1(a)) with occasional stops over ∼20 min to record the spectra (figure 2). In run 1, the pressure was decreased using a 0.25 GPa h^{-1} rate and increased using a 0.2 GPa h^{-1} rate, whereas the corresponding rates in the second run were 0.4 and 0.3 GPa h^{-1}, respectively. These higher rates were used to decrease the risk of crystallization into ice Ic, which may form under these conditions. As can be seen in figure 1(a), both runs yielded similar results. Results for C' at high frequencies should be a good indicator of the density changes. Thus, on pressure decrease, the rHDA transforms to a state of much lower high frequency C', which shows that the density decreases significantly. On pressure increase, C' increases in a two step sequence, superimposed on a gradual increase of C', which is due to the volume decrease associated with the sample compressibility. The value for C' at 1.1 GPa, i.e. at the end of the pressurization run, agrees to within 1% with that found for C' of rHDA after ice Ih had been amorphized by pressurization to about 1.2 GPa at 130 K. Figure 1(b) shows values for the dielectric permittivity ε' calculated from the values in figure 1(a) assuming isotropic compression of all the materials between the plates of the parallel plate capacitor (and also the PEEK spacers, see the experimental details), which was calculated using data for ice. For example, a ∼30% volume decrease, as for the amorphization of ice Ih into rHDA at 130 K (1.06 cm^3 g^{-1} to 0.75 cm^3 g^{-1}), yields ∼10% decrease of the interplate distance. This calculation will give a rather rough estimate of ε' as the exact dimensional

changes of the capacitor are unknown. The values obtained for the high frequency ε' of the rHDA state near 1 GPa in two different experiments were 5–8% higher than those obtained in a single experiment using a concentrical capacitor [12]. In the latter case, the dimensional changes can be ignored if the pressure is hydrostatic. (Thus, the assumption probably gives slightly too large values for the permittivity and loss, and a reasonable estimate of the inaccuracy in the permittivity is 10%.) The density data used for calculation of ε' on pressure increase at ∼130 K were taken from Loerting *et al* [28], which were measured at 125 K. The two sigmoidal increases observed in both C' and ε' reflect volume decreases associated with transformations, i.e. densifications in addition to that associated with the compressibility. The first and most pronounced increase is observed at the known LDA to HDA transition [16, 17], which occurs near 0.4 GPa as shown in figure 1(c) by previously measured data for the thermal conductivity [17]. On further pressure increase, the sample in run 1 crystallized at 0.7 GPa, whereas the other run shows a second (stretched) sigmoidal increase of C' with onset near 0.8 GPa. As shown in figure 1(c), this increase occurs at about the same coordinate as the ice Ic to rHDA transition [16, 17, 29]. As discussed previously [29, 30], ice Ic can form under similar conditions as those of LDA ice. Consequently, one possibility is that rHDA transforms to a mixture of LDA and ice Ic on depressurization to 0.03 GPa. It follows that the transformation sequence on pressurization up to 1.1 GPa would be LDA + ice Ic to rHDA + ice Ic at 0.45 GPa and rHDA + ice Ic to rHDA at 0.8 GPa. However, the transformation coordinates also agree very well with that observed recently on pressurization of pure LDA ice. Loerting *et al* [28] observed a transition sequence 'LDA → HDA' at 0.4 5 GPa and 'HDA → VHDA' at 0.95 GPa on isothermal pressurization of LDA at 125 K. Loerting *et al* [28] produced their LDA ice by heating of HDA at low pressures. This procedure inevitably yields LDA before transformation to Ic on further heating. Thus, the transformation sequence observed here can be the same, i.e. LDA → HDA → rHDA in the notation used here. However, since the experimental procedure used in this dielectric study does not allow the recovery of the sample at 77 K for a structural analysis, as done by Loerting *et al* [28], one cannot be certain concerning the state of the sample, but the two possibilities for the transition sequence are further evaluated in the discussion section.

The spectra recorded on pressure decrease and the subsequent pressure increase near 130 K are shown in figure 2. The values for ε' and the loss ε'' were also here calculated assuming isotropic compression of the sample between the electrodes, using literature data for density [16, 28]. The results agree well with those reported earlier, which were calculated using the same procedure [23]. The results for the rHDA show a relaxation process and the relaxation time τ is about 2 s at 132.6 K. After the transformation at low pressures, then only the high frequency wing of a process can be observed. That is, this relaxation process occurs at significantly lower frequencies or, equivalently, longer τ. This behaviour is unchanged until the sample is pressurized up to slightly below 0.4 GPa, where the low frequency ε' and ε'' increase significantly as a result of a transformation, in correspondence to the high frequency results shown in figure 1. This increase, which is both time and pressure dependent [23], is most pronounced in the 0.4–0.5 GPa pressure range. On further pressure increase, it has been shown that the low frequency loss (0.1 Hz) increases only slowly up to ∼0.8 GPa, where another abrupt increase occurs [23]. In the range 0.5–0.8 GPa, the relaxation peak that appears as a result of the transformation is relatively unchanged in size. The relaxation time agrees well with that for rHDA, but the sizes of the maximum in ε'', and the low frequency ε', are only about half of those for rHDA observed on pressure decrease. After the sample has been pressurized up to about 1 GPa, i.e. past the second transformation step, then the spectra corresponding to that of rHDA are recovered fully [23].

As discussed previously [12], the dielectric spectra of rHDA are best described by the symmetrical τ distribution function given by Cole and Cole [31]:

$$\varepsilon^*(\omega) = \varepsilon_\infty + (\varepsilon_0 - \varepsilon_\infty)/[1 + (\mathrm{i}\omega\tau_{cc})^{1-\alpha}], \qquad (1)$$

where $\omega(= 2\pi f)$ is the angular frequency, τ_{cc} is the Cole–Cole relaxation time, ε_∞ is the high frequency permittivity and $1-\alpha$ is a distribution factor with a value in the range 0–1. This was fitted to the dielectric spectrum at 0.6 GPa and 132.6 K for frequencies up to ∼1 kHz, shown in figure 3(a), yielding a distribution factor $1 - \alpha = 0.69$, $\tau_{cc} = 2.2$ s, and $\varepsilon_0 = 154$ which is in agreement with previous results [11, 12]. However, a subsequent fit of the Cole–Cole function after the pressure had first been decreased to 0.03 GPa and then increased to 0.7 GPa yielded different results. The fit yielded $1-\alpha = 0.64$, $\tau_{cc} = 4.4$ s, and $\varepsilon_0 = 76$ at 0.7 GPa and 130.3 K. The significant decrease in the loss maximum and slight increase in the distribution of τ are clearly visible in figure 3(a). The increase in τ, however, is explained fully by the slightly lower temperature by about 2 K. Previous results for $\tau(T)$ of rHDA at 1 GPa [12] show that a decrease of 2 K yields an increase of τ of slightly less than 3 s.

4. Discussion

4.1. Transition behaviour

As mentioned above, the changes in ε' and ε'' on depressurization of rHDA and the subsequent pressurization after a transformation can be explained by the findings of Loerting *et al* [28] of a transition sequence 'LDA to HDA to VHDA' on pressurization at 125 K. However, in this case LDA was made by heating HDA at low pressures, which inevitably yields pure LDA. Moreover, Loerting *et al* [28] could recover the sample to verify the sample state, which was not possible here. In this study of the permittivity, the state of the sample can be evaluated only by the transition behaviour upon pressurization and the properties of the sample. The former, however, leaves two possibilities concerning the state of the sample after the transformation upon depressurization of rHDA. The first is that pure LDA ice is produced at low pressure, and then the transition sequence on pressurization is identical to that established by Loerting *et al* [28]. However, the method of using relatively slow depressurization at 130 K

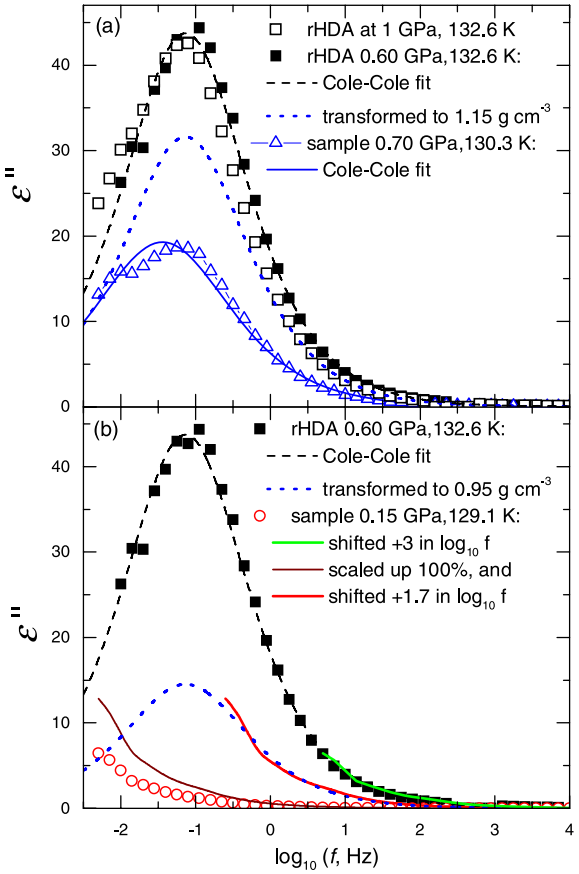

Figure 3. (a) Dielectric loss spectrum near 130 K for (■) rHDA at 0.6 GPa and (△) sample after the transformation at ∼0.03 GPa on depressurization and subsequent pressurization to 0.7 GPa via the LDA to (r)HDA transition at ∼0.45 GPa. The dotted line shows the rHDA spectrum transformed using equation (3) from a density of 1.32 to 1.15 g cm^{-3}, which occurs during this pressure cycle. (b) Dielectric loss spectrum for (■) rHDA at 0.6 GPa and (○) sample after the transformation at ∼0.03 GPa on depressurization and subsequent pressurization to 0.15 GPa. The dashed line shows the spectrum calculated from that of rHDA (0.6 GPa) using equation (3) for a density decrease from 1.32 to 0.94 g cm^{-3}, which arises during this pressure cycle.

to form LDA from rHDA, which is favourable for the study of LDA's dielectrical properties, may also produce ice Ic. We have previously reported a transition sequence 'LDA + ice Ic to HDA + ice Ic to HDA' on pressurization at ∼130 K, based on thermal conductivity data [29]. Although the thermal history of the data, shown in figure 2(c), was not identical to that used here, the results show that ice Ic can be produced under similar conditions. Thus, it is possible that rHDA transforms to a mixture of LDA and ice Ic, and that this explains the two transitions on the subsequent pressurization. The first occurs when the LDA part of the sample transforms to (r)HDA and the latter when ice Ic amorphizes. To further evaluate these possibilities, one can use the properties of the states, i.e. the variation of ε' and ε'' at the transitions.

As shown in figure 1(b), the high frequency ε' changes at the transitions, and this is partly due to the density changes. The correlation between the high frequency permittivity and the density ρ is expressed by the Clausius–Mossotti relation [32]

$$\frac{\varepsilon_\infty - 1}{\varepsilon_\infty + 2} = \frac{N_A \alpha \rho}{3\varepsilon_{vac} M} \tag{2}$$

where M is the molar mass, ε_{vac} is the permittivity of free space (8.85×10^{-12} F m^{-1}), N_A is Avogadro's number and α is the average molecular polarizability. (Equation (2) is valid for most substances and exactly for electronic polarizability, but for ice Ih ε_∞ increases slightly with increase in temperature when the density decreases.) As a very first approximation, we can assume constancy of α with pressure to evaluate the change of the high frequency ε' with density or pressure. That is, $(\varepsilon_\infty - 1)/(\varepsilon_\infty + 2) = \rho \times$ constant, and we use this to roughly estimate the high frequency ε' just below the MHz range. If one uses values for ice Ih to determine the constant ($\varepsilon_\infty = 3.1$, $\rho = 0.94$ g cm^{-3}) this yields $\varepsilon_\infty = 4.2$, 4.1, 4.5 and 5.4 for ices II, III, V and VI compared to experimental values of $\varepsilon_\infty = 4.2$, 3.5, 4.6 and 5.1 [33]. The values for the sample upon pressurization at 130 K, thus calculated, are shown in figure 1(b). Since this calculation only indicates a typical variation with density, it seems that the variation of the high frequency ε' (0.1 MHz) can be explained by the density changes observed by Loerting *et al* [28] using a similar pressurization rate. Figure 1(b) also shows results based on the density data of Mishima in the temperature range 130–140 K [16]. Only one abrupt densification is visible here, and it is due to the 'LDA to HDA' transition. However, these data were obtained using a significantly higher pressurization rate than those used here and in the work of Loerting *et al* [28].

We may then turn to the static permittivity ε_0 and its variation at the transformations. In statistical theories, ε_0 is given by the Kirkwood–Fröhlich equation [34–36] as (in SI units)

$$\frac{(2\varepsilon_0 + \varepsilon_\infty)(\varepsilon_0 - \varepsilon_\infty)}{\varepsilon_0 (\varepsilon_\infty + 2)^2} = \frac{N_A \rho}{9 M k_B T \varepsilon_{vac}} \mu_g^2 g_K, \tag{3}$$

where k_B is the Boltzmann constant, T is the temperature and μ_g is the dipole moment of an isolated molecule in the vapour phase. The quantity g_K is the orientational or dipolar correlation factor introduced by Kirkwood. It is a measure of the local ordering and the correlation of the near neighbour dipoles, given by $g_K = 1 + \Sigma_i z_i \cos\gamma_i$, where z_i is the number of correlating dipoles and γ_i is the angle between them. When g_K is greater or less than unity it indicates a predominantly parallel or antiparallel alignment of dipole vectors, respectively. Based on structural data and models, values for g_K have been calculated for both liquid water and some of the crystalline phases using statistical methods. Since the first and second neighbours are most important, the phases with strong nearest neighbour similarities are likely to have similar g_K values. For example, calculations show that the cubic and hexagonal ices have the same orientational correlation factor to within the inaccuracy of the calculation [37]. It follows that the local order similarity between LDA ice and ice I, and that between rHDA and liquid water [19], indicate that their g_K values can be similar and also that it would differ between the two amorphous states.

Also in this case we use the values for the permittivity just below the MHz range (0.1 MHz) which were measured,

as an estimate for ε_∞. (The most common and classical approach [34] is to use a value calculated from the refractive index n, i.e. $\varepsilon_\infty = n^2$, but the value for water is disputed [32], and it has been argued that it might be more appropriate to use the limiting high frequency dielectric permittivity as water and ice have absorption in the far infrared bands.) We will use it in a calculation to investigate if the state near 0.7 GPa is more probably a mixture (rHDA and ice Ic) or a HDA state. In the latter case, the state densifies to rHDA on further pressurization. If the correlation factor is unaffected by a change in density, then the change in the static permittivity can be calculated from this equation. However, as discussed further below, this is unlikely to be the case and the equation will probably give a too large density dependence. Thus, the values for of ε'' and ε', calculated using this procedure, are probably the smallest possible values.

The loss spectrum for rHDA at 0.6 GPa 132.6 K, measured on decreasing pressure, was thus transformed to a lower density using equation (3). The lower density is that of the sample after the pressure had first been decreased down to 0.03 GPa, and then increased up to 0.7 GPa 130.3 K. Results of Mishima in the range 130–140 K [16] yield $\rho = 1.32$ g cm^{-3} for rHDA at 0.6 GPa (on pressure decrease), and data of Loerting *et al* [28] yield $\rho = 1.15$ g cm^{-3} at 125 K and 0.7 GPa (on pressure increase). The procedure used to estimate the change in the loss spectrum due to this density decrease was (i) to calculateg_K for the rHDA state at 0.6 GPa using the measured value for ε_∞ and the fitted value for ε_0 (Cole–Cole function), then (ii) use equation (3) to calculate ε_0 pertaining to the lower density (1.15 g cm^{-3}) using the measured value of ε_∞ for the spectrum at 0.7 GPa, and finally (iii) calculate the spectrum of rHDA pertaining to $\rho = 1.15$ g cm^{-3} using the fitted values of the Cole–Cole function (0.6 GPa, 132.6 K), but with the measured value of ε_∞ and the calculated value of ε_0.

The calculated spectrum for rHDA at 0.7 GPa is shown in figure 3(a). Although ε'' decreases significantly as a result of the density decrease, it cannot fully explain the low loss of the measured spectrum at 0.7 GPa and 130.3 K. There are two possible explanations for this remaining difference: (i) either the Kirkwood orientational correlation factor decreases as a result of the density decrease or (ii) the sample is a mixture of rHDA and ice Ic.

In the case (i), the correlation factor must have decreased by about 30% when the density decreased from 1.32 to 1.15 g cm^{-3}, which can be deduced from equation (3). A decrease of g_K would be the normal behaviour of e.g. alcohols [38], but the opposite of that found for liquid water at high temperatures. A combination of data for the compressibility [39] and the pressure dependence of g_K for liquid water at 10 °C [40] yields $(\mathrm{d}\ln g_K/\mathrm{d}\ln\rho) = -0.4$. That is, for the density decrease here, g_K would increase by 5%. Moreover, measured data for ε_0 at 1 GPa and 0.6 GPa at 132.6 K, shown in figure 3(a), indicate that ε_0 decreases slightly with increasing pressure, which would mean that g_K decreases with increasing density, i.e. the same behaviour as water at high temperatures. In fact, the density dependence of g_K would be even more pronounced than that for liquid water, as the data yield $(\mathrm{d}\ln g_K/\mathrm{d}\ln\rho) = -1.5$. The uncertainties in these calculations are significant, but it is obvious that the change in the size of ε'' cannot be explained unless g_K of HDA is significantly smaller than that of rHDA, which seems not to be the case. The experimental behaviour for ε_0 of rHDA in the range 0.6 to 1 GPa indicates instead that the orientational correlation factor increases with decreasing density.

In case (ii), the sample must contain a mixture of ice Ic and rHDA ice to account for the much smaller loss peak at 0.7 GPa. To get an approximate value for the composition of the mixture we can assume that the loss in rHDA is roughly independent of density, as indicated by the experimental data, and that the mixture can be modelled as two capacitors with dielectric of ice Ic and rHDA, respectively, acting in parallel. It then follows that the mixture should contain about 50% rHDA.

It is difficult to verify either of these two possibilities (i) or (ii) with certainty without the possibility of x-ray analysis. The agreement with the density data of Loerting *et al* [28] and the reproducibility during two runs indicate that the observed transition sequence [28] was repeated here, whereas the agreement with the transition behaviour for ice Ic provides evidence for a mixed sample. The small ε'' and ε_0, and the somewhat broader distribution of relaxation times, also provide support for a sample mixture of LDA and ice Ic, which has implications on the analysis of the LDA dielectric properties. We can conclude that the two possible transition sequences imply that the sample contains ∼50% or 100% LDA, respectively, on pressurization up to ∼0.4 GPa, where LDA transforms to (r)HDA on further pressurization. Moreover, even if the sample is a mixture of LDA and ice Ic, the relaxation time of rHDA is unaffected at 0.7 GPa, which shows that the rHDA domain size is large. It follows that τ of LDA must also be unaffected by any presence of ice Ic. However, as discussed below, the analysis to estimate τ of LDA ice is influenced by the amount of ice Ic, if any, present in the sample.

4.2. The relaxation time of the amorphous ices

The relaxation time of LDA and rHDA ices and the nature of the relaxation processes are important in the discussion of the two liquid model of water. If a normal, i.e. not orientational, glass transition of LDA can be established, then this would provide support for the two liquid model. Results for rHDA ice [11, 12] show that τ is shorter but fairly close to that estimated for amorphous solid water (ASW) and hyperquenched glassy water (HGW). At 1 GPa, τ becomes a few seconds at 130 K, whereas that of ASW and HGW at atmospheric pressure is estimated as 2–55 s at 136 ± 1 K, and reasonable estimates for the distribution of relaxation times yield a value in the middle of this range [41]. Moreover, τ of rHDA is virtually pressure independent. The value obtained here at 132.6 K and 0.6 GPa ($\tau = 2$ s) is almost the same as that at 1 GPa ($\tau = 3$ s, figure 3(a)), which is consistent with the weak pressure dependence of the viscosity observed for liquid water at high temperatures [42, 43]. Unfortunately, water crystallizes at high temperatures, where the viscosity is much too low to firmly establish a qualitative agreement.

As can be seen in the results observed here, there is probably a relaxation process in LDA ice, but the relaxation

time cannot be established with certainty as only the high frequency wing of the process occurs within the frequency window. However, to roughly estimate the relaxation time of LDA ice, one can use the superposition principle based on the results for rHDA ice, where the loss peak is observed. The change in magnitude of the loss peak must, however, be accounted for, which can be done through equation (3) using g_K of rHDA and LDA. One extreme assumption is that LDA ice is a low density version of rHDA ice, having the same Kirkwood correlation factor. This most likely underestimates the size of the LDA loss since rHDA has an unusually small g_K. The value of g_K for ice I is significantly larger than that of rHDA ice, and since LDA ice has considerable nearest neighbour similarities with ice I it probably has a similar g_K, which thus is much larger than that of rHDA. This means that τ is longer than that estimated here based on this assumption. For example, if g_K of LDA is twice as large as that for rHDA, which is the difference between ice Ih at atmospheric pressure and rHDA at 1 GPa [12], tests show that τ of LDA will be about three times larger than that estimated here. Thus, the transformation of the spectrum for rHDA to that expected for LDA, using equation (3) with constant g_K, provides a limit for the smallest possible loss and static permittivity of LDA, which is useful in an estimation of the shortest possible τ of LDA.

The results for rHDA at ∼132.6 K and 0.6 GPa were transformed to ∼30% lower density using the value for g_K of the rHDA state. This was done using the same procedure as described above in (i)–(iii) with the modification that the values were adjusted to the density of LDA instead, i.e. a change from $\rho = 1.32$ g cm^{-3} (rHDA at 0.6 GPa) to $\rho = 0.94$ g cm^{-3} (LDA at 0.15 GPa). The results of this calculation are shown in figure 3(b). To obtain a lower limit of the relaxation time, it was further assumed that the sample contained only 50% of LDA, in accordance with the calculations above, and the measured loss was increased correspondingly to account for this. Subsequently, the measured spectrum of LDA, adjusted for the possible ice Ic content, was shifted onto the transformed rHDA spectrum, by a shift of 1.7 in the logarithmic frequency scale. It follows that the superposition of the LDA spectrum on the rHDA spectrum indicates that τ of LDA is about two orders of magnitude longer than that of rHDA. That is, since τ of rHDA is of order of 1 s at 130 K, τ of LDA is of order of 100 s. The exact value obtained from the shift in frequency is $\tau = 110$ s.

Another extreme assumption to estimate the loss magnitude in LDA ice is to use the observed density dependence for ε'' of rHDA ice, and extrapolate this to the density of LDA ice. As shown in figure 3(a), the loss size is almost the same at 1 and 0.6 GPa at 132.6 K, which corresponds to the densities 1.37 and 1.32 g cm^{-3} [16], respectively. The loss actually increases slightly with decreasing density. This has been noticed before for rHDA for a change from 1.15 to 0.45 GPa at 130 K [12], but the small increase is probably within the uncertainty as the dimensional change of the capacitor is difficult to calculate accurately. An unchanged loss size at the transformation implies three times larger orientational correlation factor for LDA than rHDA, which can be deduced from equation (3). If it is further assumed that the sample consists of 100% LDA then one obtains a limit for the longest τ. The data show a shift in the logarithmic frequency scale of 3, which yields $\tau = 10^3$ s (2200 s).

The value for the relaxation time in the 10^2–10^3 s range shows that τ of LDA ice is significantly longer than that of rHDA ice. The implication of this result is that a glass transition of LDA ice would occur at a higher temperature than that of rHDA ice. This is a surprising result, as the density of rHDA ice is ∼30% higher than that of LDA ice. A possible explanation of these seemingly inconsistent results of simultaneously decreasing density and orientational mobility can be linked to the well established local order similarities of LDA ice and ice I. The relaxation time of LDA is probably shorter than that of ice Ic under the same conditions. Isobaric results for ε'' at constant frequency (0.3 Hz) [23] show that the loss decreases at the LDA to ice Ic transition and, thus, τ of LDA ice should probably be somewhat shorter than that of ice Ic and Ih. (Ices Ic and Ih have identical dielectric properties [46].)

In the case of ice I, the reorientational motions are restricted by the 'ice rules' in the tetrahedrally coordinated ice structure [44]. Each of the four bonds exhibits two proton sites and, according to the ice rules, these are occupied so that there are two protons adjacent to each oxygen and one proton on each bond. This imposes strong limitations on the orientational mobility and the necessity of defects, such as Bjerrum defects, vacancies, and grain boundaries, for reorientational relaxation. To elaborate, to fulfil the ice rules in crystalline ice, a reorientation of one H_2O would require a long sequence of consecutive reorientations of neighbouring molecules until a lattice defect is encountered, which makes the relaxation sluggish and strongly affected by defects. In fact, it has been shown that the relaxation process in ice I is governed by Bjerrum defects [45], i.e. a double occupation of protons (Bjerrum D-defect) or absence of protons (Bjerrum L-defect) at the two proton sites between two neighbouring oxygens. In the low temperature regime below about 220 K, well purified single crystals seem to show the longest τ, whereas impure and polycrystalline samples have shorter τ. The fact that τ of ice I varies a lot dependent on the defect density makes a comparison between τ of LDA ice and ice I unfair unless the sample histories are identical. The number of Bjerrum defects varies with the initial sample purity as well as with the manner in which ice I is produced, which can change both the number of structural defects and the purity. This was shown by Gough and Davidson [46], who found that ice Ih formed from liquid water can have much shorter τ than ice Ih obtained via a high pressure phase, which they attributed to precipitation of ionic impurities in high pressure ice phases. Upon heating of ice Ih these dissolve in the lattice, which increases the number of Bjerrum defects and, consequently, τ then decreases with both time and temperature. Gough and Davidson [46] did not measure τ down to 130 K, but extrapolated values for samples produced from high pressure phases yield $\tau > 10^4$ s. (This is in strong contrast with $\tau \sim$ 40–60 s at 130 K [47–49] for ice Ih obtained by freezing from the liquid, which yields a sample with significantly more defects.) This result is

consistent with τ of LDA ice being in between that for rHDA and ice I, produced from a high pressure phase. Moreover, the demonstrated strong effect of the ice rules in prolonging τ offers a convincing explanation for the significant increase of τ at the rHDA to LDA ice transition despite decreasing density.

An interesting feature of the ice I relaxation, related to the discussion above, is the substantial decrease of τ if a small amount of certain dopants is introduced in the lattice. For instance, KOH, RbOH and HF doping are now known to alter the rate of orientational diffusion of water molecules in ice I and promote an ordering transition into ice XI at low temperatures [50, 51]. The dopant introduces defects that relax the effect of the ice rules and therefore decrease τ [48]. (The efficiency of a dopant in decreasing τ and inducing the ordering transition is not the same. For example, HF is very efficient in decreasing τ but not efficient in promoting the ordering transition [52].) Johari *et al* [53] have noticed a somewhat similar behaviour for LDA ice in a study using HF, NH_3 and NH_4F as dopants. They did not detect any changes for NH_3 and NH_4F, but HF caused a glass transition anomaly observed in a pure sample to become undetectable. In this context, it should be noted that some ionic impurities segregate from the high pressure forms of ice [46, 54], and that the effect on the orientational diffusion is dependent on the ionic impurity. For example, NH_4F does not induce an ordering transition in ice Ih [55]. Furthermore, Johari *et al* [53] observed that deuteration shifted a glass transition anomaly to higher temperatures for LDA (∼4 K), an effect observed also for ice Ih but with a larger shift of ∼15 K [56], whereas it was found to be significantly less pronounced for HGW (1 K) [53]. These results indicate that the dopant can alter the relaxation behaviour of LDA ice, and also that it has a response to deuteration similar to, but less pronounced than, that of ice Ih. These results corroborate the interpretation that the ice rules are significant for the LDA ice relaxation behaviour.

The finding that the recovery of the ice rules can explain the significant increase of τ at the rHDA to LDA transition has implications on the LDA structure. In order for the ice rules to be effective, the size of ordered domains, in which the H_2O molecules must fulfil the ice rules, must be large. Otherwise, τ would not be prolonged. It has been shown that only 10^{-7} mol of HF dopant in ice Ih is needed to reduce τ by more than an order of magnitude already at 200 K [57], and this reduction becomes several orders at low temperature. Although the number of dopant molecules is small it is still larger than the intrinsically created equilibrium Bjerrum defects, which vary with temperature and have a number density of 2×10^{-7} mol/mol of H_2O at 263 K [58]. As the thermally created Bjerrum defects decrease with decreasing temperature, extrinsically created defects, i.e. non-equilibrium defects such as grain boundaries and those created by sample impurities, will govern the relaxation also in an undoped ice samples at low temperatures, which is known to occur below about 220 K. At 220 K, the intrinsically created Bjerrum defects can be estimated to be 10^{-9} mol/mol of H_2O, which agrees well with the observation that 10^{-8} mol HF per mol of H_2O yielded only a slight decrease of τ near 220 K [57]. These results can be used to estimate the smallest defect-free domains needed for the ice rules to strongly affect the relaxation time. Thus, turning the argument of the extent of action using the HF dopant, it seems necessary to have defect-free domains involving more than 10^7 H_2O molecules for the ice rules to be very effective in prolonging τ. Since the volume of one water molecule is slightly larger than 30 $Å^3$, this indicates that domain sizes must be 10^5 nm^3.

The results for LDA ice can also be compared to that of ice I obtained by cooling the liquid. In this case, τ of LDA is slightly longer than that of the crystalline ices, which is about 60 s [47–49]. If τ of LDA is indeed governed by the ice rules, it means that the defect density for LDA, produced from a high pressure state (rHDA), is less than that for ice I obtained from the liquid. In view of the previous findings of structural and vibrational similarities between LDA ice and ice I [19, 59], and their almost identical density, such a comparison seems relevant. It follows that the size of the ordered domains must be of about the same size as those for ice I. This finding must, however, be reconciled with the structural data, which show a typical amorphous pattern [2]. Thus, LDA ice must exhibit a tetrahedrally hydrogen bonded network, which is defect free in large domains but lacks long-range translational periodicity. Still it is not obvious that such an amorphous network can explain the crystal-like phonons and thermal conductivity observed for LDA ice [17, 24, 60], but the dielectric results of LDA are certainly consistent with this crystal-like behaviour as τ seems prolonged by the effect of the hydrogen atom distribution according to the ice rules.

5. Conclusions

The dielectric spectra, in the range 5 mHz to 0.1 MHz, measured on decreasing pressure at ∼130 K down to 0.03 GPa, and subsequent increasing pressure up to 1.1 GPa show that rHDA ice and LDA ice exhibit significantly different dielectric behaviour. The rHDA ice shows a pronounced relaxation process with a relaxation time of a few seconds at 130 K. The dielectric behaviour of rHDA is similar to that of liquid water, e.g. an only weakly pressure dependent relaxation time, a pressure induced decrease of the Kirkwood orientational correlation factor, and only slightly shorter relaxation time than that estimated for hyperquenched glassy water. The spectra for LDA ice, however, show only the high frequency wing of a relaxation process under the same temperature and pressure conditions. A rough estimate using superposition of spectra indicates that the relaxation time of LDA ice is in the range 10^2–10^3 s at 130 K and 0.15 GPa, which is about two orders of magnitude longer than that for rHDA ice (∼2 s). The large increase of the relaxation time at the rHDA to LDA transition is opposite to that expected considering only the density differences between the two states. The large decrease in density of ∼30% should normally increase the orientational mobility. This result indicates that the ice rules, which limit the relaxation rate in crystalline ices, are effective also in LDA ice. Dopant and deuteration effects on the relaxation behaviour of LDA corroborate this interpretation. Thus, the near neighbour environment of LDA ice should be similar to that in the crystalline ices, which agree with structural and

spectroscopic data. Moreover, as the ice rules must involve many nearest neighbours to be effective in prolonging the relaxation time, it also indicates an extended order or, at least, an extended defect-free tetrahedrally coordinated hydrogen bonded network. These dielectric results for LDA ice are fully consistent with previous results for the thermal conductivity of LDA ice [17], which show crystal-like phonon behaviour.

Acknowledgments

This work was supported financially by the Swedish Research Council and The Faculty of Science and Technology, Umeå University.

References

[1] Mishima O, Calvert L D and Whalley E 1984 *Nature* **310** 393
[2] Mishima O, Calvert L D and Whalley E 1985 *Nature* **314** 76
[3] Johari G P and Andersson O 2007 *Thermochim. Acta* **461** 14
[4] Loerting T and Giovambattista N 2006 *J. Phys.: Condens. Matter* **18** R919
[5] Koza M M, Geil B, Schober H and Natali F 2005 *Phys. Chem. Chem. Phys.* **7** 1423
[6] Andersson O and Johari G P 2004 *J. Chem. Phys.* **121** 3936
[7] Johari G P and Andersson O 2004 *J. Chem. Phys.* **120** 6207
[8] Johari G P and Andersson O 2006 *Phys. Rev.* B **73** 094202
[9] Koza M M, Hansen T, May R P and Schober H 2006 *J. Non-Cryst. Solids* **352** 4988
[10] Loerting T, Salzmann C, Kohl I, Mayer E and Hallbrucker A 2001 *Phys. Chem. Chem. Phys.* **3** 5355
[11] Andersson O 2005 *Phys. Rev. Lett.* **95** 205503
[12] Andersson O and Inaba A 2006 *Phys. Rev.* B **74** 184201
[13] Salzmann C G, Loerting T, Klotz S, Mirwald P W, Hallbrucker A and Mayer E 2006 *Phys. Chem. Chem. Phys.* **8** 386
[14] Mishima O 1996 *Nature* **385** 546
[15] Tulk C A, Benmore C J, Urquidi J, Klug D D, Neuefeind J, Tomberli B and Egelstaff P A 2002 *Science* **297** 1320
[16] Mishima O 1994 *J. Chem. Phys.* **100** 5910
[17] Andersson O and Suga H 2002 *Phys. Rev.* B **65** 140201
[18] Finney J L, Bowron D T, Soper A K, Loerting T, Mayer E and Hallbrucker A 2002 *Phys. Rev. Lett.* **89** 205503
[19] Finney J L, Hallbrucker A, Kohl I, Soper A K and Bowron D T 2002 *Phys. Rev. Lett.* **88** 225503
[20] Klotz S, Hamel G, Loveday J S, Nelmes R J, Guthrie M and Soper A K 2002 *Phys. Rev. Lett.* **89** 285502
[21] Klotz S, Strässle Th, Nelmes R J, Loveday J S, Hamel G, Rousse G, Canny B, Chervin J C and Saitta A M 2005 *Phys. Rev. Lett.* **94** 025506
[22] Martonak R, Donadio D and Parrinello M 2005 *J. Chem. Phys.* **122** 134501
[23] Andersson O 2007 *Phys. Rev. Lett.* **98** 057602
[24] Andersson O and Inaba A 2005 *Phys. Chem. Chem. Phys.* **7** 1441
[25] Andersson O, Sundqvist B and Bäckström G 1992 *High Pressure Res.* **10** 599
[26] Forsman H 1989 *J. Phys. D: Appl. Phys.* **22** 1528
[27] Andersson O, Johari G P and Suga H 2004 *J. Chem. Phys.* **120** 9612
[28] Loerting T, Schustereder W, Winkel K, Salzmann C G, Kohl I and Mayer E 2006 *Phys. Rev. Lett.* **96** 025702
[29] Johari G P and Andersson O 2007 *Phys. Rev.* B **76** 134103
[30] Andersson O and Suga H 2005 *Netsu Sokutei* **32** 232
[31] Cole K S and Cole R H 1941 *J. Chem. Phys.* **9** 341
[32] Hill N E, Vaughan W E, Price A H and Davies M 1969 *Dielectric Properties and Molecular Behaviour* (London: Van Nostrand-Reinhold)
[33] Wilson G J, Chan R K, Davidson D W and Whalley E 1965 *J. Chem. Phys.* **43** 2384
[34] Kirkwood J G 1939 *J. Chem. Phys.* **7** 911
[35] Fröhlich H 1949 *Theory of Dielectrics* (Oxford: Clarendon)
[36] Böttcher C J F 1973 *Theory of Electric Polarization* 2nd edn vol 1 (Amsterdam: Elsevier)
[37] Rahman A and Stillinger F H 1972 *J. Chem. Phys.* **57** 4009
[38] Hiejima Y and Yao M 2003 *J. Chem. Phys.* **119** 7931
[39] Fine R A and Mirrero F J 1973 *J. Chem. Phys.* **59** 5529
[40] Srinivasan K R and Kay R L 1974 *J. Chem. Phys.* **60** 3645
[41] Johari G P 2005 *J. Chem. Phys.* **122** 144508
[42] Worrell F T 1965 *Nature* **207** 620
[43] DeFries T and Jonas J 1977 *J. Chem. Phys.* **66** 896
[44] Bernal J D and Fowler R H 1933 *J. Chem. Phys.* **1** 515
[45] Geil B, Kirschgen T M and Fujara F 2005 *Phys. Rev.* B **72** 014304
[46] Gough S R and Davidson D W 1970 *J. Chem. Phys.* **52** 5442
[47] Johari G P and Whalley E 1981 *J. Chem. Phys.* **75** 1333
[48] Kawada S 1988 *J. Phys. Soc.* **57** 3694
[49] Haida O, Matsuo T, Suga S and Seki S 1974 *J. Chem. Thermodyn.* **6** 815
[50] Tajima Y, Matsuo T and Suga H 1982 *Nature* **299** 810
[51] Tajima Y, Matsuo T and Suga H 1984 *J. Phys. Chem. Solids* **45** 1135
[52] Johari G 1998 *J. Chem. Phys* **109** 9543
[53] Johari G P, Hallbrucker A and Mayer E 1991 *J. Chem. Phys.* **95** 6849
[54] Suga H, Matsuo T and Yamamuro Y 1992 *Pure Appl. Chem.* **64** 17
[55] Matsuo T and Suga H 1987 *J. Physique* **48** C1 477
[56] Suga H 1983 *Pure Appl. Chem.* **55** 427
[57] von Hippel A, Mykolajewycz R, Runck A H and Westphal W B 1972 *J. Chem. Phys.* **57** 2560
[58] Johari G P 2000 *Chem. Phys.* **258** 277
[59] Kolesnikov A I, Li J, Parker S F, Eccleston R S and Loong C-K 1999 *Phys. Rev.* B **59** 3569
[60] Schober H, Koza M M, Tölle A, Masciovecchio C, Sette F and Fujara F 2000 *Phys. Rev. Lett.* **85** 4100